

High-Resolution Gamma Spectroscopy in the Decay of $^{231}\text{Pa}^\dagger$

A. G. de Pinho, E. F. da Silveira, and N. L. da Costa

Department of Physics, Pontificia Universidade Católica, Rio de Janeiro (ZC-20), Brasil

(Received 9 February 1970)

The decay of ^{231}Pa was reinvestigated by means of Ge(Li) singles and coincidence techniques. Our best spectrometer showed a resolution (full width at half maximum) of 850 eV for the 300-keV γ rays. 78 γ rays were attributed to the decay of ^{231}Pa . A level scheme for ^{227}Ac was proposed and interpreted in terms of rotation bands. Alternating terms in the $K=\frac{3}{2}$ bands were discussed in connection with Coriolis coupling to $K=\frac{1}{2}$ bands.

I. INTRODUCTION

The complexity of the conversion-electron and γ -ray spectra following the α decay of ^{231}Pa has been long recognized.^{1,2} Until now, the most complete investigation of the α spectrum of this nuclide is due to Baranov *et al.*,³ who identified 18 α branches, furnishing a solid basis for a decay scheme. These authors have also studied internal-conversion electrons, and they obtained results in reasonable agreement with data previously reported by Falk-Vairant, Teillac, and Victor^{1,2} and Stephens.⁴ The first attempt to analyze the complex γ peak observed by scintillation techniques in the energy range of 300 keV was due to Foucher.⁵ In the energy range from 250 to 400 keV, many γ rays were observed which are due to deexcitation of the rotation band favored in the α decay of ^{231}Pa .

Later, dePinho⁶ and his co-workers of the Orsay group,^{7,8} investigating both conversion-electron and γ spectra, identified many other transitions. In particular, the following transitions were reported: 259.1, 272.7, 282.6, 299.2, 301.7, 312.5, 329.6, 331.0, 342.9, 353.5, 356.4, 378.4, and 422 keV. The measurement of the absolute internal-conversion coefficient in the K shell was also reported⁶ for a number of γ rays, and especially the more intense transitions of 283, 299, 302, and 329 keV were established, on the basis of the measured α_K , as $E1$, $M1 (+E2)$, $E1$, and $M1 (+E2)$, respectively. These results combined with lifetime measurements⁷ have permitted the correct assignment of the parities of the low-lying levels of ^{227}Ac . In fact, as suggested by Stephens, Asaro, and Perlman⁹ and by Baranov *et al.*,³ the rotation band based on the level at 329 keV of excitation has the same intrinsic Nilsson configuration as the ground state of ^{231}Pa , namely, $K=\frac{1}{2}^- [530]$. Thus the parity of the ground state of ^{227}Ac was fixed unambiguously as negative. The parities of the levels at 27.5, 30.0, and 46.5 keV were fixed as +, -, and +, respectively.

More recently, Lange, Hagee, and McCarthy¹⁰

observed some new γ rays with energies 244, 409, 437, 439, 488, 513, and 517 keV, and Hagee *et al.*¹¹ remeasured, with more precise techniques, the K -shell internal-conversion coefficient of the 329-keV transition. Their results are $\alpha_K=0.41 \pm 0.05$ and $e_K/e_{L1}=3.85 \pm 0.38$, confirming the results given in Ref. 6, $\alpha_K=0.24 \pm 0.12$ and $e_K/e_L=3.7 \pm 0.5$.

Some details of the low-energy γ spectrum are also given in Ref. 6. It is worth noting that a relatively strong γ transition of 46 keV was identified. This energy agreed very well with the energy of the most intensely populated level in the α decay. This transition, unobserved in the electron spectrum, was then tentatively assigned as $E1$, and its presence confirmed the assignment of a positive parity to that level.

While the present work was in course, Lange and Hagee¹² published a more complete study of this γ spectrum using Ge(Li) and Si(Li) detectors. Even if some general results are in good agreement, there are very important differences between our results and those presented in Ref. 12.

In order to obtain additional information about this interesting decay scheme, the γ spectrum was studied again employing a higher resolution than hitherto reported. Special attention was paid to the presence of oscillating terms in the rotation bands based on the ground and first excited states.

Some partial results of this work were previously reported.¹³

II. EXPERIMENTAL TECHNIQUES

A. Source Preparation

The ^{231}Pa source furnished by the Radiochemical Center, Amersham, England, was in the oxide form.

A procedure due to Kirby and Figgins¹⁴ was used to prepare radiochemically pure ^{231}Pa sources. The protactinium oxide was dissolved in hot concentrated H_2SO_4 , and the solution was diluted to 18 $M\text{H}_2\text{SO}_4$. After cooling, an equal volume of solution of 12 $M\text{HCl}$ was added with some drops of

30% H₂O₂. The aqueous solution was extracted with 2 ml of diisobutyl carbinol diluted to 50% with benzene. The ²³¹Pa, free of descendants, stays in the organic phase.

An alternative method¹⁵ of radiochemical purification of ²³¹Pa was employed. We added 5 mg of Fe⁺⁺⁺ carrier to the diluted sulfuric acid solution of protactinium and then precipitated by the addition of NH₄OH. The protactinium and its descendants (except Ra) are carried by the iron precipitate. After a centrifugal separation, the precipitate was dissolved to 1 M HNO₃ - 0.02 M HF and added to a column of Dowex 50 - X4 (400 mesh). On elution with three column volumes of the same solvent, Pa free of descendants passed through the column.

Both methods give very good results, but the second one is more practical for further repurifications.

B. Detectors and Electronics

The γ ray spectrum covering an energy range from 10 to ~ 600 keV was studied with two separate spectrometer systems, one specially designed for the x-ray region.

The detector of the x-ray spectrometer (ORTEC, model No. 8213-08) consists of a nearly cylindrical volume of lithium-compensated germanium (~0.4 cm³) with a surface-barrier contact (≈ 150 Å of gold) as the entrance window for the radiation. The detector is kept in a cryostat with a beryllium window 0.25 mm thick. An integral cryogenic preamplifier, a shaping amplifier (440 A) and baseline restorer (438) complete the system. The detector was operated at 940 V and the total system resolution, measured with an Intertechnique 4096-channel pulse-height analyzer, was of 500 eV full width at half maximum (FWHM) for the 14.38-keV γ rays of ⁵⁷Co and 950-eV FWHM for the 279.19-keV γ rays of ²⁰³Hg.

The second spectrometer system used a 2-cm³ Ge(Li) detector consisting of a planar diode with a depletion depth of 4 mm (model No. 8045). The associated electronics (Tennelec, TC 135 FET preamplifier and TC 200 amplifier) showed a photopeak of about 2.0 keV FWHM for the 121.98-keV γ rays of ⁵⁷Co. The gain of the amplifiers was chosen in such a way that we get typical values of 0.04 to 0.2 keV/channel in all the spectra. The best resolution at low rates was obtained with the first differentiator and integrator time constants set a 1.6 μ sec and the second differentiator time constant at 1 msec. In order to avoid attenuation by the germanium dead layer, the low-energy part of the spectrum was observed with the source at the side of the detector. The active solution was

put into a glass ring around the detector. A region especially difficult to analyze is that around 140 keV, because of the coalescence of the backscatter peaks and the Compton edges of the intense group of transitions with energies from 250 to 380 keV.

The high precision in the energy determination, attained with the x-ray spectrometer, required special care in obtaining the energy versus channel function. The nonlinearity of the amplifier-analyzer system was measured with a commercial precision pulser (model No. 419) and γ -ray standards. The pulser was coupled to the preamplifier through the test input with the detector connected and bias applied. The curve showing the deviation from linearity had a nearly parabolic shape. The same result was obtained with the standard γ rays using either the position of the interpolated maximum of the photopeaks or a Gaussian fit to the symmetric part of the peak.

C. Detector Calibration and Efficiency Determination

Both spectrometers were finally calibrated with the γ energy standards (²⁴¹Am, ¹⁰⁹Cd, ⁵⁷Co, ¹⁹⁸Au, ²⁰³Hg, ⁵¹Cr, ⁷Be, ¹³⁷Cs, ¹³³Cs, ¹³¹I, ²³⁰Th, ²¹⁰Pb, and the x rays of Ac, Ba, Ag, Pb, Tl, Hg, and Np). These data were used to establish an energy-calibration function consisting of a linear term and a quadratic term which represented nonlinearities in the system. The energies of the most prominent γ rays of ²²⁷Ac were determined within 30 eV below 100 keV and within 60 eV around 300 keV.

Relative intensities of γ rays were obtained from photopeak areas, taking into account the relative photopeak efficiency. The latter was established by observing the spectra of sources that emit γ rays of several different energies with well-known intensity ratios. For the region from 6 to 100 keV the efficiency curve was mainly determined from the relative photopeak areas of the γ ray and the x ray and the reported internal-conversion coefficients and fluorescent yields. When the source decayed by electron capture, corrections were made. This method is essentially the pair-point method; the relative positions of groups of related points were adjusted graphically until a smooth curve could be drawn through them. The areas of the peaks were obtained after a graphical determination of a smooth curve, in general a straight line, separating from the total spectral distribution that part of the distribution which was to be considered the peak. After subtracting this background, the full-energy-peak profiles were compared with standards profiles. Distinct efficiency-versus-energy functions were obtained for the different detectors and geometries used. A typical uncertain-

ty of about 10–20% in the relative γ intensities was obtained for the γ rays of ^{227}Ac with energies below 100 keV. Around 300 keV, these uncertainties were reduced by a factor of 2.

D. Coincidence Measurements

Coincidence runs were performed with both $\text{Gi}(\text{Li})$ detectors or with one of them and a 7.6-cm \times 7.6-cm or a 2.5-cm \times 0.6-cm $\text{NaI}(\text{Tl})$ scintillation counter. The detectors were placed at right angles with a Cu-Pb-Cu shield between them to prevent scattering from one detector to the other. Crossover coincidence timing was employed, with a resolving time between 40 and 80 nsec, in order to avoid the loss of coincidences by variations of crossover times. Chance coincidences were obtained and subtracted. The use of two analog-to-digital converters made it possible to operate in the two-parameter mode. Typical configurations were 16×256 and 32×128 channels.

III. EXPERIMENTAL RESULTS

A. Singles Spectra

The singles spectra for the decay of ^{231}Pa obtained with the x-ray spectrometer are shown in Figs. 1, 2, and 3. The portion of the recorded

spectrum with energy above 400 keV is shown in Fig. 4. Especially worth noting are the many closely spaced doublets that are almost separated; for instance, 27.35–29.95, 299.94–302.52, and 327.02–329.89 keV. Even at this high resolution, however, we believe that other even more complex peaks remain unfolded, for example, the 57.2-keV peak. Graphical analyses were made in these cases to determine the components.

A list of all the γ rays assigned to the decay of ^{231}Pa is given in Table I. The relative intensities are normalized about the 27.35-keV peak. Not all the lines could be fitted into a decay scheme. In the final column of the table the letters A and NA indicate those that could and could not be so accommodated.

The region below 27 keV is difficult to analyze, partly because of the secondary effects of the intense line of 27.35 keV, but mainly because of the problem of sorting out the L x-ray lines of the daughter Ac.

B. Measurements in the L X-Ray Region

An attempt was made to reconstruct the L x-ray spectrum based on the relative intensities given by Powers¹⁶ and our own efficiency curve. The $L\alpha$ group is much simpler than the $L\beta$ and $L\gamma$ groups.

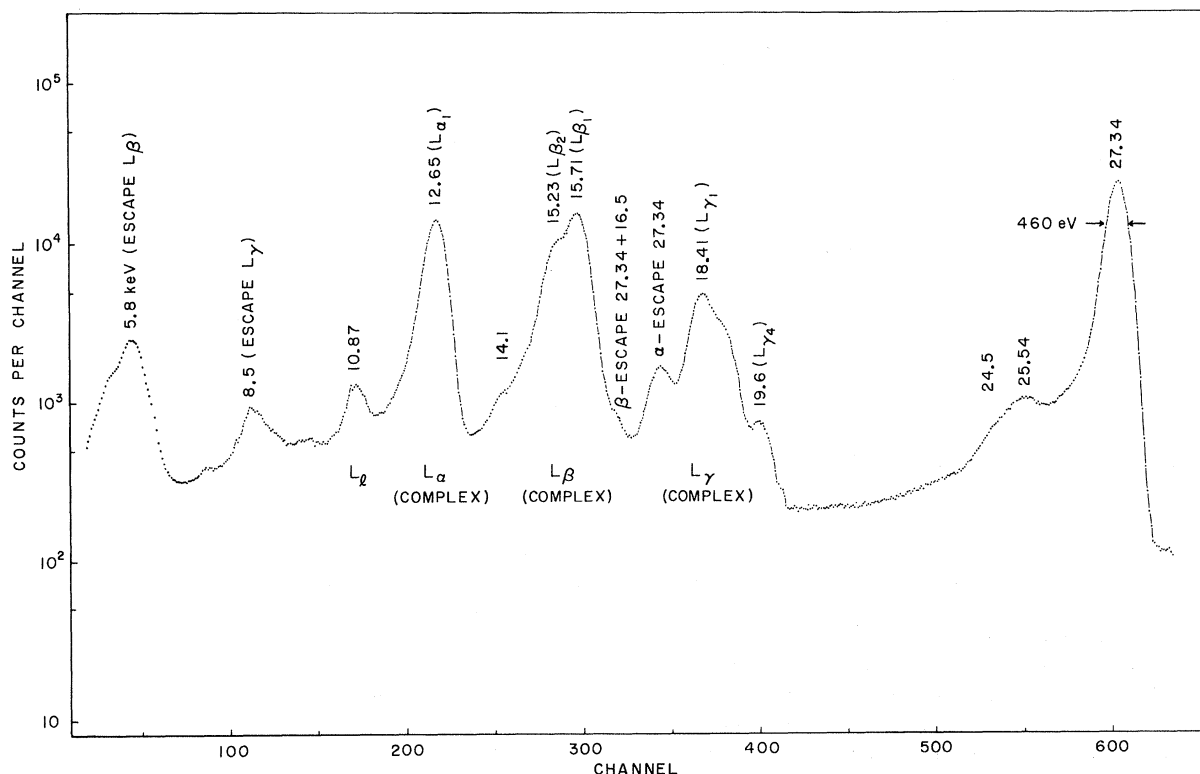


FIG. 1. The L x-ray region of the γ spectrum. In this portion of the spectrum the resolution (FWHM) is about 450 eV.

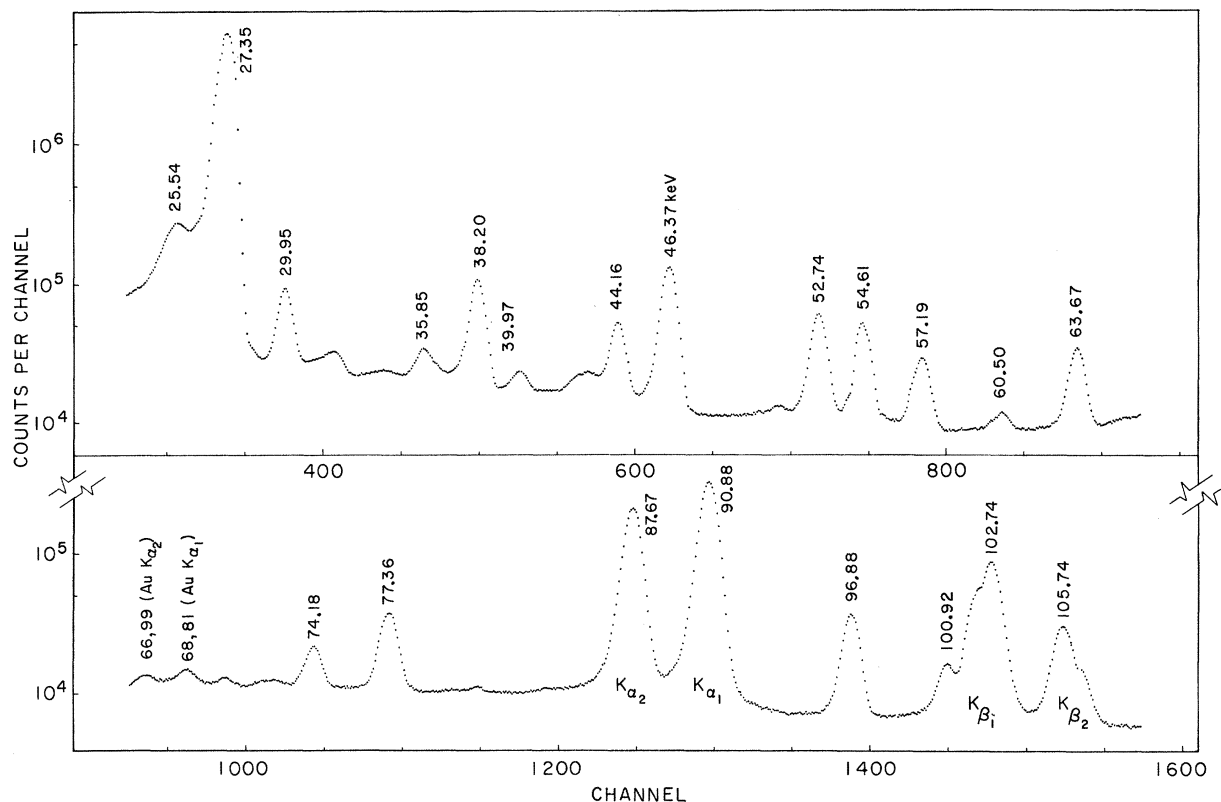


FIG. 2. Typical low-energy portion of the γ -ray spectrum of ^{231}Pa as obtained with the x-ray spectrometer.

In our spectrum, a peak at 12.65 keV combines the $L\alpha_1$ and $L\alpha_2$ lines in the ratio of 100:11. This peak was used to normalize the total spectrum once the Compton continuum was subtracted. No agreement was reached for the shapes of the total relative intensities for the $L\beta$ and $L\gamma$ groups. An even stronger disagreement was encountered for the $L\ell$ transition.

Since direct measurements of excited x rays in Ac are unfeasible, the L x-ray spectra of neighboring heavy elements were investigated in several ways in order to determine by interpolation the lines for Ac. First, the transitions following internal conversion were studied in the cases following α decay; ^{230}Th and ^{241}Am , and β decay; ^{210}Pb and ^{203}Hg . Secondly, the spectrum of transitions following external conversion due to 662-keV photons were examined for the cases of Pb, Bi, Th, and U. For both of these approaches the Ge(Li) spectrometer was employed, and the profile of the 14.38-keV γ ray of ^{57}Co was used as the standard. Special care was taken with backscattering effects which, at these low energies, correspond to a tail in the photopeaks strongly dependent on energy.

Finally, a plane one-crystal Philips spectrometer was used to determine more precisely the L

x-ray spectra of Pb, Bi, Th, and U. The equipment consisted of a 2-kw x-ray generator (100-kV, type PW 1310), an x-ray tube with gold anode (PW 2161/00), a vacuum spectrometer (PW 1540) with target holder, and a fine collimator (160 μ spacing). A topaz analyzing crystal ($2d = 2.712 \text{ \AA}$) was used in connection with a motor-driven goniometer (PW 1050/25). In the crystal chamber a flow proportional counter detects the low-energy radiation. A beryllium window scintillator was also used.

The relative L x-ray yield depends on the mode of vacancy production, being different for internal conversion, capture, and photoprocesses. In internal conversion, the number of conversions in the L subshells is dependent on the multipolarity of the γ transitions. Given the complexity of conversion processes in the L subshells of Ac, it is likely that the intensity distribution in this case would approach that produced by external conversion, but this remains a hazardous statement. At best, the method employed shows the presence of the most prominent γ rays with energies less than 21 keV; these γ rays appear in the experimental spectra after the subtraction of the constructed L x-ray spectrum duly normalized at the 12.65-keV peak.

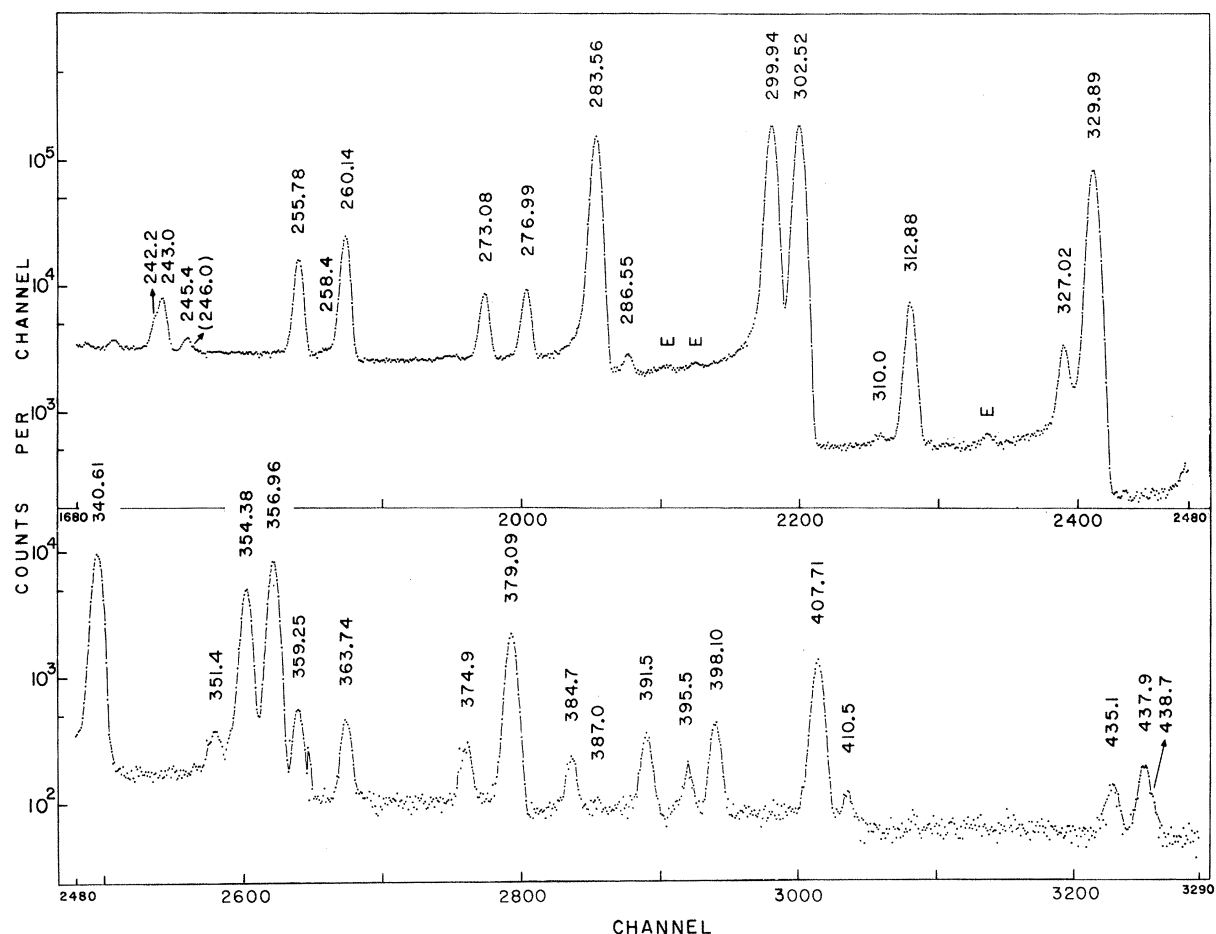


FIG. 3. Singles γ -ray spectrum of ^{231}Pa from 200 to 450 keV. In this region the resolution (FWHM) is better than 1 keV.

The interpolated relative intensities of the Ac L x rays obtained and used in this work are given in Table II. In Table III the same results are presented for the K x rays.

C. Coincidence Results

Interesting results appear when the lower portion of the energy spectrum is measured in coincidence with the entire region of the spectrum above 85 keV. The coincidence spectrum is given in Fig. 5. With all K x rays eliminated, the γ spectrum in the lower portion is revealed in greater clarity, making it possible to determine which states are directly populated from the higher levels. The relative weakness of the transitions associated with the $K = \frac{3}{2}^+$ is evident, indicating a preference for the $K = \frac{1}{2}^-$ band to decay to the negative-parity $\frac{3}{2}^-$ band. The presence, in the coincident spectrum, of a relatively intense 57.1-keV transition does not invalidate this statement, since there are two transitions separated by about 100 eV; one is an intraband transition in the $\frac{3}{2}^+$ band and the other, less

intense, is an intraband transition in the $\frac{1}{2}^-$ band.

The spectrum of lines in coincidence with the very intense 27.35-keV γ ray shows many interesting features (Fig. 6). Using the NaI crystal to gate the pulses, the minimum window width was 4 keV and thus not all 25- and 30-keV γ rays were completely excluded. The 2-cm³ Ge(Li) crystal was used as detector, and coincidence involving γ rays above 380 keV were not observed, because of poor statistics. The width of the complex peak at 300 keV is reduced by a factor of 2, clearly showing the disappearance of the 299.94-keV transition, as previously reported.⁶ Other lines which disappear are the following: 329.89, 354.38, 356.96, 255.78, and 260.14 keV. Lines which appear in coincidence are 283.56 and 340.61 keV. In addition, a complex peak about 244 keV and a very weak transition of about 277 keV are seen. The presence of the 283.56-keV line in coincidence indicates the presence of a very important 18.99-keV transition, which probably corresponds to that of 18.88 keV reported by Stephens. This transition must be highly converted and the direct observation of the γ rays

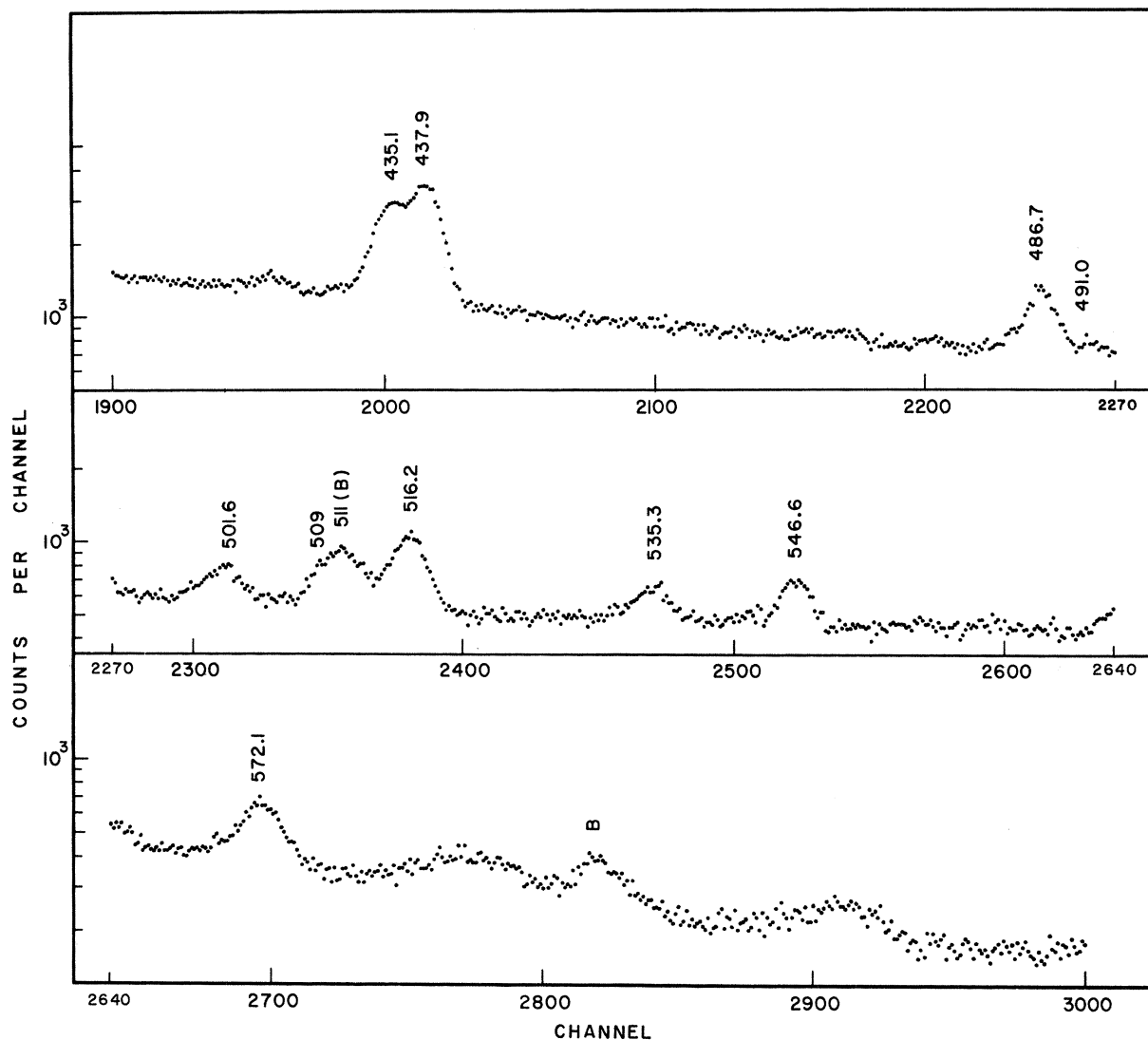


FIG. 4. High-energy portion of the γ -ray spectrum of ^{231}Pa recorded with a large-volume Ge(Li) detector. B means that the peak is present in the background spectrum.

is rendered difficult by the presence of the $L\gamma$ complex group with about the same energy. However, even in the singles spectra the presence of γ rays in excess over the expected $L\gamma$ x-ray peak is beyond any doubt. This transition is a very important piece in building up a coherent decay scheme, since it corresponds, probably, to more than 30% of the disintegrations.

With the x-ray spectrometer the following lines were seen to be in coincidence with the 27.35-keV γ rays: 25.5, 38.2, 57.2, 63.7, and 77.4 keV. There is also evidence for a 102-keV transition partially unresolved from the $K\beta'_1$ x-ray group. Moreover, the peak at 19 keV becomes as important as those corresponding to the $L\alpha$ and $L\beta$

groups, confirming the presence of γ rays of about this energy in coincidence with the 27.35-keV transition.

In coincidence with the 283.6-keV line we observed the 27.35-keV γ ray, the L x-ray group, and the 46.37-keV γ ray. In addition, a very weak line of 57 keV was seen; evidence of the presence of the intraband $\frac{7}{2}^- \rightarrow \frac{3}{2}^-$ transition in the $K = \frac{1}{2}^-$ band. When the gate is displaced towards the complex 300–302-keV peak, the 29.95-keV line appears as a satellite of the 27.35-keV peak. The 46.37-keV line disappears, but vestiges of a peak remain at 57 keV. This last peak is the only one that appears in coincidence with the 330-keV line.

Additional results of the coincidence experiments

TABLE I. Energies (in keV) and relative intensities of the γ rays attributed to the decay of ^{231}Pa . The intensities are arbitrarily normalized to $I_\gamma(27.3 \text{ keV}) = 1000$. In the last column, A and NA indicate those transitions that could and could not be accommodated in the proposed level scheme; ($i \rightarrow j$) means a transition from level i to level j as indicated in Fig. 7.

Energy (keV)	Relative photon intensity	Observations
10.9 \pm 0.1	\sim 40	$L\ell$
12.65 \pm 0.01	\sim 800	$L\alpha$
14.1 \pm 0.1		NA
15.7	\sim 1000	$L\beta$
16.5 \pm 0.1		A (4 \rightarrow 3)
18.5	\sim 250	$L\gamma$
\sim 19 (18.88 ^a)		A (4 \rightarrow 2)
24.5 \pm 0.1	\sim 1	A (15 \rightarrow 14)
25.54 \pm 0.06	\sim 10	A (7 \rightarrow 6)
27.35 \pm 0.02	1000	A (2 \rightarrow 1)
29.95 \pm 0.02	9.9 \pm 0.9	A (3 \rightarrow 1)
31.00 \pm 0.05	1.0 \pm 0.2	NA
31.54 \pm 0.05	0.7 \pm 0.2	NA
35.82 \pm 0.03	1.7 \pm 0.2	A (7 \rightarrow 5)
38.20 \pm 0.02	16.0 \pm 1.6	A (6 \rightarrow 4)
39.57 \pm 0.04	0.15 \pm 0.07	NA
39.97 \pm 0.02	1.3 \pm 0.2	NA
42.48 \pm 0.05	0.6 \pm 0.1	NA
43.05 \pm 0.05	0.7 \pm 0.2	NA
44.16 \pm 0.02	6.5 \pm 0.7	A (5 \rightarrow 3)
46.37 \pm 0.02	22.4 \pm 0.2	A (4 \rightarrow 1)
50.98 \pm 0.05	0.15 \pm 0.06	A (18 \rightarrow 16)
52.74 \pm 0.02	9.1 \pm 0.9	A (8 \rightarrow 5)
54.61 \pm 0.02	8.7 \pm 0.8	A (6 \rightarrow 3)
56.76 \pm 0.04	0.6 \pm 0.1	NA
57.19 \pm 0.03	4.2 \pm 0.4	A (6 \rightarrow 2)
60.50 \pm 0.03	0.7 \pm 0.1	A (9 \rightarrow 8) ^b
63.67 \pm 0.03	5.4 \pm 0.5	A (7 \rightarrow 4)
70.50 \pm 0.05	0.7 \pm 0.1	NA
71.9 \pm 0.1	0.2 \pm 0.1	A (10 \rightarrow 8) ^b
72.5 \pm 0.1	0.4 \pm 0.2	A (12 \rightarrow 10) ^b
74.18 \pm 0.04	2.7 \pm 0.3	A (5 \rightarrow 1)
77.36 \pm 0.03	7.3 \pm 0.8	A (9 \rightarrow 7) ^b
87.67 \pm 0.02	61 \pm 5	$K\alpha_2$
90.88 \pm 0.02	103 \pm 8	$K\alpha_1$
96.88 \pm 0.03	9.5 \pm 1.0	A (8 \rightarrow 3)
100.92 \pm 0.04	3.4 \pm 0.5	A (11 \rightarrow 7)
\sim 102.6 (102.55 ^a)	\sim 2	A (9 \rightarrow 6) ^b
102.7 \pm 0.1	38.5 \pm 3.0	$K\beta'_1$
105.7 \pm 0.1	11.5 \pm 1.5	$K\beta'_2$
124.6 \pm 0.1	0.5 \pm 0.2	A (10 \rightarrow 5)
144.5 \pm 0.1	1.3 \pm 0.4	A (12 \rightarrow 8)
199 \pm 1	0.6 \pm 0.2	NA
242.2 \pm 0.1	0.9 \pm 0.1	NA
243.0 \pm 0.1	3.7 \pm 0.3	A (13 \rightarrow 3) ^b
245.4 \pm 0.1	0.8 \pm 0.1	NA
246.0 \pm 0.2	$<$ 0.1	A (13 \rightarrow 2) ^b
255.78 \pm 0.07	10.9 \pm 0.6	A (14 \rightarrow 5)
258.4 \pm 0.1	0.25 \pm 0.06	NA
260.14 \pm 0.08	18.6 \pm 1.1	A (16 \rightarrow 8)

TABLE I (Continued)

Energy (keV)	Relative photon intensity	Observations
273.08 \pm 0.09	6.2 \pm 0.3	A (13 \rightarrow 1) ^b
276.99 \pm 0.09	7.2 \pm 0.4	A (16 \rightarrow 7)
283.56 \pm 0.06	169 \pm 8	A (14 \rightarrow 4)
286.55 \pm 0.10	1.0 \pm 0.1	NA
299.94 \pm 0.06	244 \pm 14	A (14 \rightarrow 3)
302.52 \pm 0.06	252 \pm 14	A (14 \rightarrow 2)
310.0 \pm 0.1	0.15 \pm 0.05	NA
312.88 \pm 0.08	10.2 \pm 0.6	A (16 \rightarrow 5)
327.02 \pm 0.10	3.2 \pm 0.2	A (15 \rightarrow 2)
329.89 \pm 0.06	140 \pm 7	A (14 \rightarrow 1)
340.61 \pm 0.07	17.8 \pm 0.9	A (16 \rightarrow 4)
351.4 \pm 0.1	0.38 \pm 0.04	A (17 \rightarrow 5)
354.38 \pm 0.08	10.2 \pm 0.6	A (15 \rightarrow 1)
356.96 \pm 0.07	18.6 \pm 1.1	A (16 \rightarrow 3)
359.25 \pm 0.10	0.97 \pm 0.08	A (19 \rightarrow 7)
363.74 \pm 0.10	0.80 \pm 0.07	A (18 \rightarrow 5)
374.9 \pm 0.1	0.50 \pm 0.04	NA
379.09 \pm 0.08	5.3 \pm 0.4	A (17 \rightarrow 4)
384.7 \pm 0.1	0.44 \pm 0.04	A (19 \rightarrow 6)
387.0 \pm 0.1	0.05 \pm 0.02	A (16 \rightarrow 1)
391.5 \pm 0.1	0.73 \pm 0.06	A (18 \rightarrow 4)
395.5 \pm 0.1	0.28 \pm 0.03	A (17 \rightarrow 3)
398.10 \pm 0.08	1.00 \pm 0.08	A (17 \rightarrow 2)
407.71 \pm 0.06	3.9 \pm 0.3	A (18 \rightarrow 3)
410.5 \pm 0.1	0.20 \pm 0.02	A (18 \rightarrow 2)
435.1 \pm 0.1	0.36 \pm 0.04	A (20 \rightarrow 5) ^b
437.9 \pm 0.1	0.44 \pm 0.04	A (18 \rightarrow 1)
438.7 \pm 0.1	0.16 \pm 0.04	NA
486.7 \pm 0.3	0.19 \pm 0.04	A (22 \rightarrow 3) ^b
491.0 \pm 0.6	0.05	A (23 \rightarrow 5) ^b
501.6 \pm 0.5	0.06 \pm 0.02	A (20 \rightarrow 1) ^b
509 \pm 1	0.03 \pm 0.01	NA
516.2 \pm 0.6	0.14 \pm 0.03	A (22 \rightarrow 1) ^b
535.3 \pm 0.7	0.05 \pm 0.02	A (23 \rightarrow 3) ^b
546.6 \pm 0.7	0.06 \pm 0.02	A (24 \rightarrow 3) ^b
572.1 \pm 0.8	0.05 \pm 0.02	NA

^aValue taken from Ref. 4.

^bAssignment is uncertain.

are presented in the next sections.

D. Conversion Coefficients

We have calculated the absolute values of the K -shell coefficients of the most-intense transitions in the 260–380-keV range. They are based on reported relative conversion-electron intensities,⁶ on the absolute K -shell conversion coefficient of the 329-keV transition,¹¹ and on the relative photon intensities determined in this work. These α values are given in Table IV with the predominant multipole attributed to each transition, after comparison with theoretically derived values.¹⁷

The L -shell conversion coefficients for some transitions below 100 keV were calculated on the

TABLE II. Determined relative intensities of some L x-ray lines in ^{227}Ac . These intensities are obtained by interpolation as described in the text.

L x rays	Energy (keV)	Relative intensity
$Ll, L_{III}M_I$	10.87	5 ± 1
$L\alpha_2, L_{III}M_{IV}$	12.50	11 ± 1
$L\alpha_1, L_{III}M_V$	12.65	100
$L\beta_6, L_{III}N_I$	14.60	3.0 ± 0.7
$L\beta_4, L_I M_{II}$	15.18	8 ± 2
$L\beta_2, L_{III}N_V$	15.23	37 ± 3
$L\beta_1, L_{II}M_{IV}$	15.71	80 ± 7
$L\beta_5, L_{III}O_{IV}$	15.79	7 ± 1
$L\beta_3, L_I M_{III}$	15.93	7 ± 1
$L\gamma_1, L_{II}N_{IV}$	18.41	21 ± 3
$L\gamma_2, L_I N_{II}$	18.76	4 ± 1
$L\gamma_3, L_{II}O_I$	18.81	
$L\gamma_3, L_I N_{III}$	18.95	
$L\gamma_6, L_{II}O_{IV}$	19.00	6 ± 1
$L\gamma_4, L_I O_{II}$	19.63	2.0 ± 0.5

TABLE III. Relative intensities of the most important K x-ray lines of ^{227}Ac .

K x rays	Energy (keV)	Relative intensity
$K\alpha_2, L_{II}K$	87.67	59 ± 4
$K\alpha_1, L_{III}K$	90.88	100
$K\beta_3, M_{II}K$	102.05	11.3 ± 1.5
$K\beta_1, M_{III}K$	102.85	25.0 ± 2.5
$K\beta_5, \left\{ \begin{array}{l} M_{IV}K \\ M_VK \end{array} \right\}$	$\left\{ \begin{array}{l} 103.39 \\ 103.54 \end{array} \right\}$	0.71 ± 0.08
$K\beta_2^{II}, N_{II}K$	105.68	2.7 ± 0.3
$K\beta_2^I, N_{III}K$	105.87	5.5 ± 0.6
$K\beta_4, N_{IV}K$	106.10	0.6 ± 0.1
$O_{II}K$	106.54	1.8 ± 0.2
$O_{III}K$	106.59	

basis of electron intensities given by Baranov, the α_L value of the 27.35-keV transitions, and the γ intensities given in this work. Asaro *et al.*¹⁸ reported $\alpha_L(27.35 \text{ keV}) = 2.8 \pm 0.3$. The value determined in the present work is 3.0 ± 0.3 . Adopting this latter value we found the results given in Table V.

To determine more precisely the L -shell con-

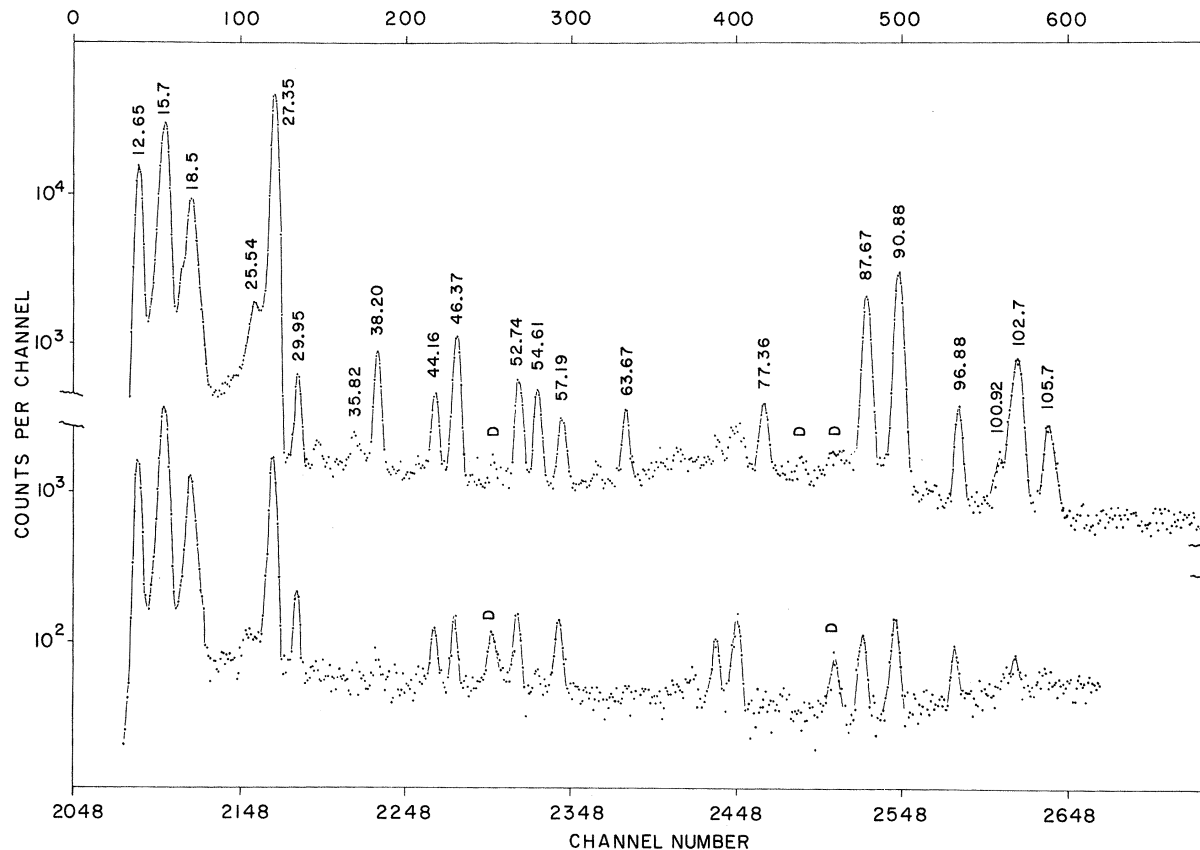


FIG. 5. Low-energy spectrum in coincidence with all the γ rays with $E > 85$ keV. Chance coincidences were not subtracted. This spectrum was obtained with an "old" source, and many daughter activities are present. The corresponding peaks are indicated by a D. The upper curve is a direct spectrum.

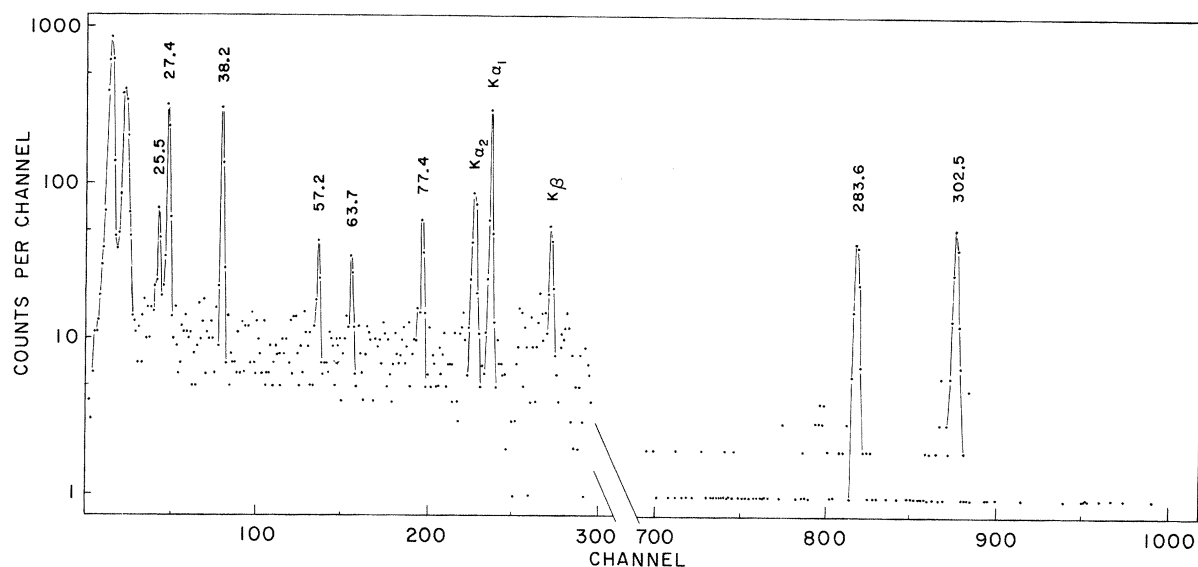


FIG. 6. γ spectrum in coincidences with the 27.35-keV line. Chance coincidences were not subtracted.

version coefficient of the 29.95-keV transition, the following coincidence measurement was performed. With the 2-cm³ detector used for gating the analyzer, the window of the discriminator was placed in such a way that only the upper part of the complex 299.94–302.52-keV peak could authorize the passage of pulses from the x-ray spectrometer. In this situation we observed only the 27.35-keV γ rays and L x rays in the ratio

$$(L \text{ x ray})/\gamma(27.35) = \alpha_L(27.35)\omega_L = 1.35,$$

after correcting for efficiencies. With the fluorescent yield $\omega_L = 0.45$ we find $\alpha_L(27.35) = 3.0$ with an estimated error of 10%. The ω_L value adopted by Asaro *et al.*¹⁸ was 0.52. With $\omega_L = 0.45$ they would find $\alpha_L = 3.16$.

The base line was then moved down, and the complete complex peak passed through the gate. The 29.95-keV γ rays appeared in the coincident spectrum with an intensity only 42 ± 5 times less than that of the 27.35-keV γ rays. In these spectra the L x-ray peaks were approximately twice as high, and the $L\alpha : L\beta : L\gamma$ ratios were slightly modified. We finally found

$$(L \text{ x ray})/\gamma(27.35) = 2.79.$$

The 312.77-keV γ rays also passed by the gate, but the contribution of this line to the coincident spectrum can be separately obtained by moving up the base line of the gate to eliminate completely the complex peak around 300 keV. This procedure also gives information on coincidences with the

TABLE IV. Measured α_K values of some transitions observed in the decay of ²³¹Pa.

Transition energy (keV)	Relative K-electron intensity	Relative photon intensity (present work)	α_K	Predominant multipole
260.14	12 \pm 2	18.6 \pm 1.1	0.62 \pm 0.16	M1
273.08	2.5 \pm 1.0	6.2 \pm 0.3	0.39 \pm 0.14	M1 + E2
283.56	7.0 \pm 1.5	169 \pm 8	0.04 \pm 0.01	E1
299.94	100 \pm 8	244 \pm 14	0.39 \pm 0.06	M1
302.54	10 \pm 2	252 \pm 14	0.038 \pm 0.010	E1
312.88	5.0 \pm 1.5	10.2 \pm 0.6	0.47 \pm 0.16	M1
329.89	60 \pm 6	140 \pm 7	0.41 \pm 0.05 ^a	M1
340.61	1.0 \pm 0.4	17.8 \pm 0.9	0.054 \pm 0.020	E1 or E2
354.38	1.5 \pm 0.5	10.2 \pm 0.6	0.14 \pm 0.05	M1 + E2
356.96	7.5 \pm 1.5	18.6 \pm 1.1	0.39 \pm 0.10	M1
379.09	1.0 \pm 0.4	5.3 \pm 0.4	0.18 \pm 0.08	M1 + E2

^aSee Ref. 11.

TABLE V. Measured α_L values of some low-energy transitions observed in the decay of ^{231}Pa .

Transition energy (keV)	exp	α_L theor ^a	Multipolarity
27.35	3.0 ± 0.3	2.7(E1)	E1
29.95	220 ± 40	100(M1), 2800(E2)	M1+E2 (~4%)
38.20	70 ± 12	44(M1), 835(E2)	M1+E2 (~3%)
57.18	105 ± 18	117(E2)	E2
63.67	76 ± 13	74(E2)	E2
96.88	9.8 ± 1.6	9.6(E2)	E2

^aSee Ref. 17.

Compton background in the region of interest. Correction for chance coincidences were also made. We finally found, as an average of two different determinations

$$\alpha_L(29.95) = 140 \pm 20,$$

indicating an almost pure M1 transition. This result does not agree with that obtained from the relative electron intensities given by Baranov *et al.* A very small E2 contribution implies also a conflict with the L-subshell ratios given by the same authors. However, it seems to us that the 29.95-keV transition is predominantly an M1 transition

with a few percent (2 to 5%) of E2.

Table VI presents the estimated intensities of some transitions observed in the decay of ^{231}Pa calculated with the measured conversion coefficients. They are given as the number of transitions per 100 disintegrations, and an error of the order 20% is expected in the very intense low-energy transitions. For the 46.37-keV transition the theoretical value of α was used.

IV. CONSTRUCTION OF THE DECAY SCHEME

The proposed decay scheme is shown in Fig. 7, and arguments are given for its construction below.

The ground and first excited states are firmly established as the $\frac{3}{2}[532]$ and $\frac{5}{2}[651]$ Nilsson states, respectively. On the basis of our measured γ -ray energies alone, it is possible to assign nine γ rays as cascade and crossover transitions between members of rotational bands built on these states. These intraband transitions are 29.95, 44.16, 74.18, 52.74, and 96.88 keV in the negative-parity band and 57.19, 38.20, 63.67, and 25.54 keV in the positive-parity band. Moreover, four interband transitions serve to give additional information for positioning the rotational levels. These transitions are those of 27.35, 46.37, 54.61, and 35.85 keV. The 16.5-keV interband transition is very difficult

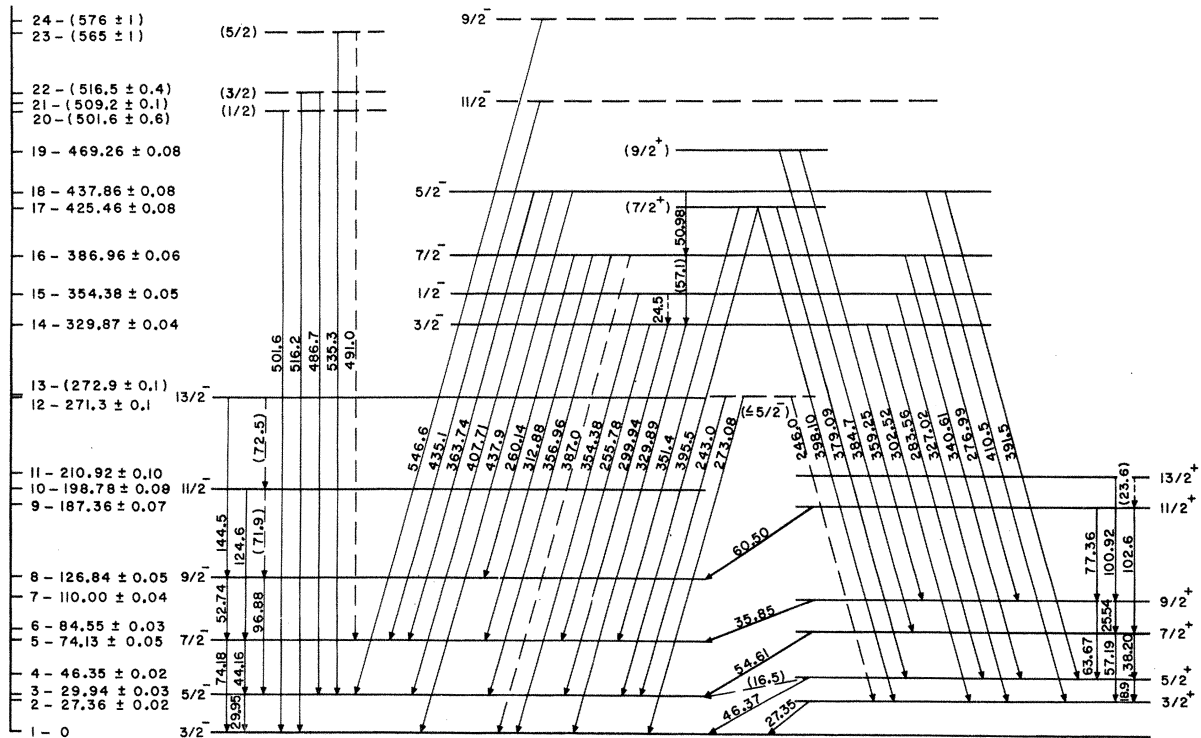


FIG. 7. Proposed level scheme for ^{227}Ac . The numbers at the left refer to the last column of Table I. All energies are given in keV.

TABLE VI. Estimated intensities (per 100 decays) of some transitions observed in the decay of ^{231}Pa . Errors are not quoted and can be as large as 20%.

Transition energy (keV)	Estimated intensity	Transition energy (keV)	Estimated intensity
27.35	46	283.56	1.4
29.95	28	299.94	2.7
38.20	14	302.52	2.1
46.37	0.4	312.88	0.14
57.18	7	329.89	1.8
63.67	6	340.61	0.14
96.88	1.3	354.38	0.1
260.14	0.3	356.96	0.2
273.08	0.1	379.09	0.06

to observe owing to the presence of one of the escape peaks of the 27.35-keV line. These results and the coincidence experiments with the 27.35-keV γ rays permit the interpretation of the eight lower-energy levels of ^{227}Ac as pertaining to two rotational bands. The energies of the strongest transitions were determined with a precision of about ± 20 eV (see Table I, column 1), and the difference in energy between the sum of any cascade transitions and the appropriate crossover transition is always consistent with our estimated experimental errors. Two additional levels in each band were determined, but with less clear-cut arguments.

The cascade and crossover transitions within a rotational band should, of course, have multipolarities of $M1 (+E2)$ and $E2$, respectively. The measured α_L values are consistent with the assignments made concerning the rotational structure of the level scheme. In the measured cases (29.95- and 38.20-keV transitions) the upper limit of the $E2/M1$ mixing ratio for the intraband cascade transitions is 5%. This ratio is considerably more important for the $M1 + E2$ interband transitions deexciting the $\frac{1}{2}[530]$ band levels. The natural explanation for this fact is that for $\frac{1}{2}[530] \rightarrow \frac{3}{2}[532]$ transitions, $|\Delta\Lambda| = 2$. Such a change in the asymptotic quantum numbers for this single-proton transition does not violate the Alaga¹⁹ selection rules in the $E2$ case, but hinders the $M1$ transition.

The $\frac{3}{2}$, $\frac{7}{2}$, and $\frac{5}{2}$ levels of the rotational band built on the $\frac{1}{2}[530]$ Nilsson orbitals are fixed by the observation of at least five transitions depopulating each one. These transitions link the $\frac{1}{2}^-$ band with the $\frac{3}{2}$ bands. The energies of these levels are then fixed within 40 to 80 eV. Levels at 354.38 ($\frac{1}{2}^-$), 425.46, and 469.26 keV are also firmly established. The first one pertains to the $K = \frac{1}{2}$ rotational band.

The observation of the intraband transitions is, in this particular case, rendered difficult by some peculiar features of the γ spectrum.

When it was possible to estimate the transition intensities, the discrepancy between the total feeding and decaying intensities was small and compatible with the α intensities reported by the Baranov group.³ The only noticeable exception is the 46.35-keV level. We estimated that this level is fed by about $(47 \pm 6)\%$ of the disintegrations. Since the direct transition to the ground state has a negligible intensity ($\sim 0.4\%$, if $E1$), this level must be deexcited via the 27.36- and/or 29.94-keV levels: It happens that the 19-keV transition cannot account for more than 35% of the disintegration, and the 16.5-keV transition, if $E1$, could not be responsible for the missing 10%. We are thus forced to postulate another low-lying level in ^{227}Ac with $E \sim 30$ keV. A level reported by the Baranov group³ with energy around 34 keV is a potential candidate for playing the role of an intermediate level in the decay of the 46.35-keV level. We were not able to identify this level. The nonobservation in the γ spectrum of the transitions responsible for the feeding and the deexcitation of this level is probably due to the fact that these transitions are strongly converted. On the other hand, the analysis of the electron lines reported in Ref. 3 is not conclusive. The very intense electron line of 14.1 keV interpreted by those authors as the conversion of a 34.1-keV transition in the L_1 subshell can also be explained as the conversion of a 19.0-keV transition in the M_1 subshell.

Some electron lines reported in Ref. 3 could be reinterpreted to explain our proposed decay scheme. For example, the 3.8-keV electron line could be originated by the L_1 conversion of the 23.6-keV transition. This transition is essential to understand the feeding of the 187.4-keV ($\frac{11}{2}^+$) level.

A reinvestigation of the low-energy conversion spectrum seems to be of considerable importance for a more complete description of the decay scheme of ^{231}Pa .

Complementary information on the level scheme of ^{227}Ac is given by the β decay of ^{227}Ra . γ rays of about 300 and 500 keV were observed^{20, 21} in addition to the very intense 27.3-keV transition. An intensity of nearly 0.6 photons of 500 keV per 100 β decays suggests the presence of a low spin level at that energy. This level could pertain to a $K = \frac{1}{2}^+$ rotational band expected in this region of energy. Some nonassigned transitions with $E > 486$ keV (see Table I) could be used to construct this band. We tentatively suggest levels at 501.6 keV ($\frac{1}{2}^+$), 516.5 keV ($\frac{3}{2}^+$), and 565.3 keV ($\frac{5}{2}^+$), accommodating five observed transitions.

V. DISCUSSION OF THE RESULTS

Coupling effects between rotational and intrinsic motions can be described in terms of the rotor model²² or, more generally, can be obtained by expanding the rotational energy as a power series of the total angular momentum.²³ In regions where the rotational picture is most applicable, the series converges rapidly, and one obtains a description of a rotational band in terms of a simple $I(I+1)$ rule [except in the special case where $K = \frac{1}{2}$ when an additional diagonal term $(-)^{I+1/2}(I+\frac{1}{2})$ is present]. ²²⁷Ac is at the border of a rotational region and relatively strong deviations from the simple rotational rules are expected in this nucleus.

It was long suggested^{8,9} that the 329.89-keV level, populated by a favored α branch, has the same configuration as the ground state of ²³¹Pa. Both levels, with spin $\frac{3}{2}$, are heads of well-developed rotational bands. The $I = \frac{1}{2}$ and $I = \frac{7}{2}$ members of this band were identified in ²²⁷Ac at energies of 354.37 and 386.86 keV, respectively. The ground state of ²²⁷Ac has measured spin $\frac{3}{2}$ and is connected to the 329.89-keV level by a $M1+E2$ transition. The ground state must therefore have odd parity and was identified^{6,7} with the $\frac{3}{2}^- [532]$ configuration. The first excited state, connected to the ground state by a very strong $E1$ transition, was identified^{6,7} with the Nilsson orbital $\frac{3}{2}^+ [651]$. The search for the higher-spin partners of the $K = \frac{3}{2}^\pm$ rotation bands was attempted by many authors^{3,6,12} but only with partial success.

A. $K = \frac{1}{2}^-$ Band

The $K = \frac{1}{2}^- [530]$ rotational band is defined by the following levels: 329.87 ($I = \frac{3}{2}$), 354.38 ($I = \frac{1}{2}$), 386.96 ($I = \frac{7}{2}$), and 437.86 keV ($I = \frac{5}{2}$).

Describing this rotation band by a three-parameter formula,

$$E(I) = AI(I+1) + (-)^{I+1/2}(I+\frac{1}{2})[A_1 + I(I+1)B_1],$$

the higher spin levels are predicted at 507.8 ± 1.2 keV ($I = \frac{11}{2}$), 570.0 ± 0.8 keV ($I = \frac{9}{2}$), 696 ± 2 keV ($I = \frac{13}{2}$), and 746.5 ± 1.8 keV ($I = \frac{15}{2}$). Baranov *et al.* observed strong evidence of α branches populating levels at 501 and 560 keV. Since all the energies in the Baranov paper seem to appear a few keV below the true values, we propose levels at 509.2 and 575.7 keV as rotational states with $I = \frac{11}{2}$ and $I = \frac{9}{2}$, respectively. These levels are associated with the 435.1-keV (509.1–74.1 keV) and 545.8-keV (575.7–29.9 keV) transitions. The parameters of this rotational band are $A = 6.89 \pm 0.02$ keV, $a = A_1/A$

$= -2.22 \pm 0.02$, and $B_1 = 89.9 \pm 4.3$ eV.

If we accept the 509.2-keV level as the $I = \frac{11}{2}$ member of this band and try to find the $I = \frac{9}{2}$ state by means of a four-parameter formula,

$$E(I) = I(I+1)[A + I(I+1)B] + (-)^{I+1/2}(I+\frac{1}{2})[A_1 + I(I+1)B_1],$$

we get $A = 6.86$ keV, $a = -2.225$, $B_1 = 83.0$ eV, $B = 2.9$ eV, and $E(\frac{9}{2}) = 571.6$ keV.

The $\frac{1}{2}^- [530]$ band occurs as the ground states of ²³¹Pa and ²³³Pa.²⁴ It is also observed in ²³⁷Np.²⁵ The rotational constants and decoupling parameters are $A = 6.34$ keV, $a = -1.40$ in ²³¹Pa; $A = 6.0$ keV, $a = -1.3$ in ²³³Pa; and $A = 6.72$ keV, $a = -1.64$ in ²³⁷Np.

It is interesting to observe that two unassigned transitions with 374.9 and 486.7 keV could reproduce Baranov's energy levels if placed between the 501.7- and 126.84-keV levels and between the 560.8- and 74.12-keV levels, respectively: The multipole character of both transitions would be $M1+E2$.

B. $K = \frac{3}{2}^-$ Band

Results for this rotational band are summarized in Fig. 8. It is described by a three-parameter formula:

$$E(I) = I(I+1)[A + I(I+1)B] + (-)^{I+3/2}(I-\frac{1}{2})(I+\frac{1}{2})(I+\frac{3}{2})A_3.$$

In the rotor model the parameter B measures the vibration-rotation coupling, and the last term is associated with the mixing with $K = \frac{1}{2}$ configurations via the Coriolis term of the Hamiltonian. In our particular case the most important coupling of this band must be with the $K = \frac{1}{2}^- [530]$ band. When we take the four lowest levels to fix these parameters we find $A = 6.04 \pm 0.01$ keV, $B = 3.2 \pm 0.6$ eV, and $A_3 = 15.8 \pm 0.5$ eV. The $\frac{11}{2}$ and $\frac{13}{2}$ levels are then calculated at 200.6 ± 0.8 and 274.1 ± 1.3 keV, respectively. We found, experimentally, levels at 198.8 and 271.3 keV with all the characteristics of $\frac{11}{2}$ and $\frac{13}{2}$ states, respectively.

The first four levels of this rotation band are firmly established. All the intraband transitions were observed. The four transitions deexciting the two higher levels are very weak, indicating, as observed, a small population of these levels. Baranov *et al.*³ reported a very weak α branch feeding a level at 268.2 keV (0.04%). It is not impossible that this level is the $I = \frac{13}{2}$ partner of the band, but the possible existence of another level

$$\begin{aligned}
 A &= 6.04 \pm 0.01 \text{ keV} \\
 B &= 3.2 \pm 0.6 \text{ eV} \\
 A_3 &= -15.8 \pm 0.5 \text{ eV}
 \end{aligned}
 \quad 3/2^- [532]$$

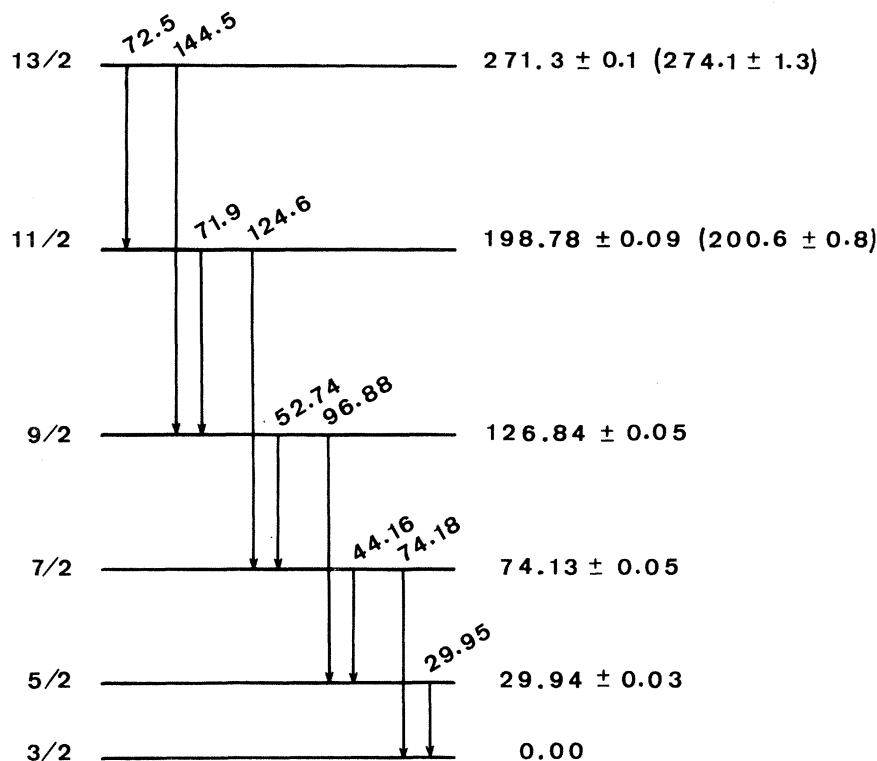


FIG. 8. The $K = \frac{3}{2}^-$ rotation band. The calculated energies of the $\frac{11}{2}^-$ and $\frac{13}{2}^-$ levels are shown in parentheses. All energies are given in keV.

at 272.9 keV (see below) renders difficult any definite conclusion, since the feeding of this last level via the 329.87-keV level implies the presence of a 57.0-keV transition. The determination of a weak transition in this range of energy is rendered difficult by the presence of a strong 57.18-keV transition.

The coincidence experiments indicate that the 260.14-keV transition is in coincidence with 52.74- and 96.88-keV γ rays, and that the 312.77-keV transition is in coincidence with the 44.16- and 74.14-keV γ rays. Following the conversion-electron studies of Stephens, $E2$ multipolarities for the 74.18- and 96.88-keV transitions are very plausible. The α_L value for the 96.88-keV transition given in Table V is that of an $E2$, in agreement with the proposed decay scheme.

C. $\frac{3}{2}^+$ Band

This positive-parity rotation band is shown in Fig. 9. The three-parameter formula in this case gives $A = 4.21 \pm 0.01$ keV, $B = 8.6 \pm 0.5$ eV, and $B_3 = -86.5 \pm 0.5$ eV. The value of the moment of inertia

is abnormally high, and the band seems very perturbed with very conspicuous alternating perturbations indicating a strong coupling with hidden $K = \frac{1}{2}^+$ bands. These bands could correspond to the $\frac{1}{2}^+ [660]$ or the $\frac{1}{2}^+ [651]$ Nilsson states. We discussed in the preceding section the possible identification of one of these bands in ^{227}Ac . The predicted levels at 190.5 ± 0.7 keV ($\frac{11}{2}^+$) and 207.4 ± 1.3 keV ($\frac{13}{2}^+$) must be identified with the experimental levels found at 187.36 ± 0.07 and 210.92 ± 0.10 keV, respectively.

The 302.52-, 283.56-, and 340.61-keV transitions depopulating the $K = \frac{1}{2}^-$ band and arriving at the $\frac{3}{2}^+$, $\frac{5}{2}^+$, and again $\frac{5}{2}^+$ states of the $K = \frac{3}{2}^+$ band, respectively, are of the $E1$ type, as indicated by the measured value of α_K (Table IV).

The levels of this band are alternately strongly and weakly populated by α decay: the $\frac{3}{2}^+$, $\frac{7}{2}^+$, and $\frac{11}{2}^+$ levels receive only about 3% of the decays, and the $\frac{5}{2}^+$, $\frac{9}{2}^+$, and $\frac{13}{2}^+$ population amounts to about 50% of the disintegrations. Such a situation agrees very well with theoretical results.²⁶

An interesting point is the intensity equilibrium at the 84.55-keV level. The population due to direct α decay is very small ($\sim 0.4\%$); on the other hand,

$$\begin{aligned}
 A &= 4.21 \pm 0.01 \text{ keV} && 3/2^+ [651] \\
 B &= 8.6 \pm 0.5 \text{ eV} \\
 A_3 &= -86.5 \pm 0.5 \text{ eV}
 \end{aligned}$$

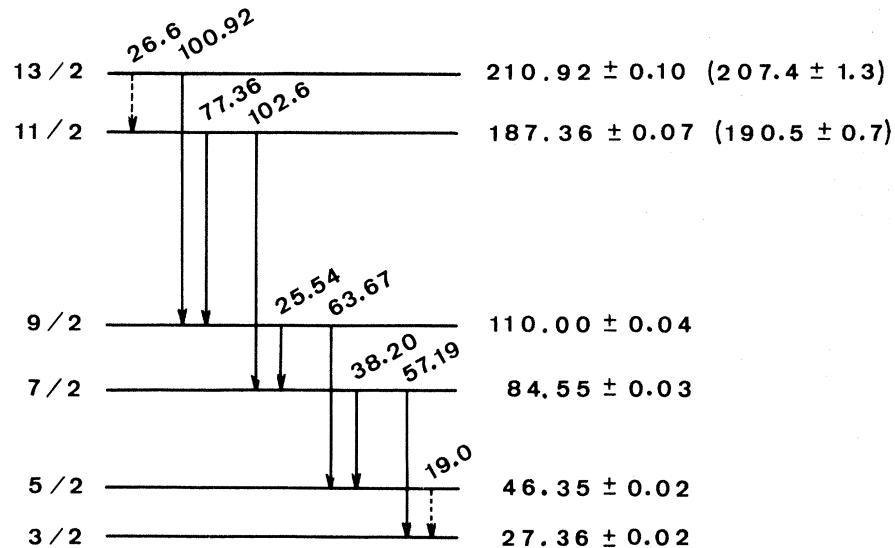


FIG. 9. The $K = \frac{3}{2}^+$ rotation band. See Fig. 8 for explanation.

we have starting at this level the very intense transitions of 57.19 and 38.20 keV, responsible for almost 20% of the disintegrations. This apparent unbalance is accounted for by the presence of the 25.5-keV intraband transition proceeding from the 110.0-keV level.

It was not possible to identify in our γ spectra a relatively weak γ line of 23.56 keV responsible for the population of the 187.38-keV level, as discussed in a previous section. On the other hand, the 100.9- and 102.7-keV transitions are well established, and their character is consistently given as $E2$ by conversion-electron data,⁴ justifying the hypothesis of a rotational band extending up to the $\frac{13}{2}$ level.

As shown in Table V, the α_L values for the 57.19- and 63.67-keV transitions are those of pure $E2$ transitions, whereas the 29.95- and 38.20-keV transitions are mixtures of $M1$ plus a few percent of $E2$, in accordance with the proposed decay scheme.

Concerning the population of the $K = \frac{3}{2}^+$ band via the $K = \frac{1}{2}^-$ band, the following results were obtained: The very intense 283.56-keV transition ($E1$) is in coincidence with the 46.37-keV γ rays which are also in coincidence with the 340.61-keV line ($E1$); the 38.20-keV transition appears in coincidence with the 276.99-keV γ rays indicating the feeding of the $\frac{7}{2}^+$ level via the $\frac{5}{2}^+$ level.

The anomalies observed in this rotation band may possibly be connected with the especially

strong Coriolis coupling which manifests itself in the large moment of inertia of this band, which is about 40% larger than for the other two bands considered. The Nilsson orbit $\frac{3}{2}[651]$ contains large components with $j = \frac{13}{2}$ (87%) for which the Coriolis matrix elements are especially large. The positive sign of the B coefficient and the importance of the alternating term reflect also the major role played by the Coriolis interaction in this band.²⁷

D. Other Levels of ^{227}Ac

Beside the 18 levels described in Secs. VA, VB, and VC classified in three rotational bands, there are a few other levels well established in the decay scheme of ^{227}Pa . A level at 425.46 keV deexcited by at least four transitions is probably represented by quantum numbers $\frac{7}{2}^+$. A direct transition from this level to the ground state was not observed. A level at 469.26 keV connected to the $\frac{7}{2}$ and $\frac{9}{2}$ levels of the $\frac{3}{2}^+$ rotation band could be a $\frac{9}{2}^+$ state. If so, we could wonder if the 425.46- and 469.27-keV levels do not pertain to a rotational band built on an intrinsic $\frac{7}{2}^+$ state or on a γ vibration associated with the $\frac{3}{2}[651]$ orbital. A value of $A = 4.87$ keV for this band would not be too different from the value obtained for the $\frac{3}{2}^+$ band. The next level ($\frac{11}{2}^+$) of this band is expected to be around 523 keV; it could be associated with the 438.7-keV transition ($\frac{11}{2}^- \rightarrow \frac{7}{2}^+$, $K = \frac{3}{2}$).

The existence of a level at 272.9 keV is also pos-

sible, but its population remains an open problem. The transition of 273.08 keV is $M1+E2$; if it corresponds to the decay of the proposed level, this will indicate negative parity for this level.

Levels possibly associated with a $K = \frac{1}{2}^+$ band were already discussed.

Finally it is interesting to point out that octupole vibrations can be important in ^{227}Ac . This kind of vibration occurs at very low energy in many nearby even- A isotopes. In particular, a well-developed odd-parity band is known in ^{226}Ra beginning at 253 keV. This vibration mode when associated with a $K\pi$ intrinsic state gives rise to a new state

with the same value of K , but opposite parity.

VI. ACKNOWLEDGMENTS

We gratefully thank Dr. T. L. Cullen, S.J. for his continued interest in this work and for many helpful comments and suggestions concerning the organization and writing of this report. We are also indebted to Mrs. T. A. Curzio for valuable assistance in processing the data and to A. M. de Souza for helping us with the plane-crystal x-ray spectrometer measurements.

†Work supported by grants from C.N. Pq. and B.N.D.E. (FUNTEC-23).

¹P. Falk-Vairant, J. Teillac, and C. Victor, *J. Phys. Radium* **13**, 313 (1952).

²P. Falk-Vairant and M. Rio, *J. Phys. Radium* **14**, 65 (1953).

³A. Baranov, V. M. Kulakov, P. S. Samoilov, A. G. Zelenkov, Y. R. Rodionov, and S. V. Pirozhkov, *Zh. Eksperim. i Teor. Fiz.* **41**, 1475 (1961) [transl.: *Soviet Phys - JETP* **14**, 1053 (1962)].

⁴F. S. Stephens, unpublished, reported by E. K. Hyde, I. Perlman, and G. T. Seaborg, *The Nuclear Properties of the Heavy Elements* (Prentice-Hall, Inc., Englewood Cliffs, New Jersey, 1964), p. 689.

⁵R. Foucher, Ph. D. thesis, University of Paris, 1961 (unpublished).

⁶A. G. de Pinho, Ph. D. thesis, University of Paris, 1963 (unpublished).

⁷H. Abou-Leila, R. Foucher, A. G. de Pinho, N. Perrin, and M. Valadares, *J. Phys. Radium* **24**, 857 (1963).

⁸R. Foucher, A. G. de Pinho, and M. Valadares, in *Proceedings of the International Congress on Nuclear Physics, Paris, France, 1964*, edited by P. Gugenberger (Centre National de la Recherche Scientifique, Paris, France, 1964), p. 62.

⁹F. S. Stephens, F. Asaro, and I. Perlman, *Phys. Rev.* **113**, 212 (1959).

¹⁰R. C. Lange, G. R. Hagee, and J. I. McCarthy, *Bull. Am. Phys. Soc.* **11**, 408 (1966).

¹¹G. R. Hagee, R. C. Lange, A. C. Barnett, A. R. Campbell, C. R. Cothorn, D. D. Griffing, and H. J. Nennecke, *Nucl. Phys.* **A115**, 157 (1968).

¹²R. C. Lange and G. R. Hagee, *Nucl. Phys.* **A124**, 412 (1968).

¹³A. G. de Pinho, E. F. da Silveira, and N. L. da Costa, in *Proceedings of the International Conference on Properties of Nuclear States, Montreal, Canada, 1969*, edited by M. Harvey *et al.* (Preses de l'Université de Montréal,

Montréal, Canada, 1969).

¹⁴H. W. Kirby and P. E. Figgins, National Research Council Report No. NAS-NS-3016, 1959 (unpublished), p. 48.

¹⁵F. Nelson, *J. Chromatog.* **16**, 538 (1964).

¹⁶M. C. Powers, *X-ray Fluorescent Spectrometer Conversion Tables for Topaz, LiF, NaCl, EDDT, and ADP Crystals* (Philips Electronics, Instrument Division, Mount Vernon, New York, 1960).

¹⁷L. A. Sliv and I. M. Band, in *Alpha-, Beta-, and Gamma-Ray Spectroscopy*, edited by K. Siegbahn (North-Holland Publishing Company, Amsterdam, The Netherlands, 1965), Vol. 2, pp. 1639-1672.

¹⁸F. Asaro, F. Stephens, J. Hollander and I. Perlman, *Phys. Rev.* **117**, 492 (1960).

¹⁹G. Alaga, *Phys. Rev.* **100**, 432 (1955); *Nucl. Phys.* **4**, 625 (1957).

²⁰J. P. Butler and J. S. Adam, *Phys. Rev.* **91**, 1219 (1953).

²¹F. S. Stephens, F. Asaro, and I. Perlman, unpublished, quoted in D. Strominger, J. M. Hollander, and G. T. Seaborg, *Rev. Mod. Phys.* **30**, 585 (1958).

²²A. Bohr, *Kgl. Danske Videnskab. Selskab, Mat.-Fys. Medd.* **26**, No. 14 (1952); A. Bohr and B. Mottelson, *ibid.* **27**, No. 16 (1953); A. Kerman, *ibid.* **30**, No. 15 (1956).

²³A. Bohr and B. R. Mottelson, *At. Energ. (USSR)* **14**, 41 (1963) [transl.: *Soviet J. At. Energy* **14**, 36 (1966)].

²⁴E. K. Hyde, I. Perlman, and G. T. Seaborg, *The Nuclear Properties of the Heavy Elements* (Prentice-Hall, Inc., Englewood Cliffs, New Jersey, 1964).

²⁵C. M. Lederer, J. K. Poggenburg, F. Asaro, J. O. Rasmussen, and I. Perlman, *Nucl. Phys.* **84**, 481 (1966).

²⁶J. K. Poggenburg, University of California, Lawrence Radiation Laboratory Report No. UCRL 16187, 1965 (unpublished).

²⁷A. Bohr and B. R. Mottelson, *Nuclear Structure* (W. A. Benjamin, Inc., New York), Vol. 2, to be published.